Temporal Evolution and Ablation Mechanism of Laser-induced Graphite Plume at 355 nm

Young-Ku Choi, Hoong-Sun Im,[†] and Kwang-Woo Jung[*]

Department of Chemistry, Wonkwang University, Iksan 570-749, Korea
[†]Korea Research Institute of Standards and Science, Taeduk Science Town, Taejon 305-600, Korea
Received September 17, 1999

Expansion dynamics of C^+ ions ejected from 355-nm laser ablation of graphite target in vacuum has been investigated by pulsed-field time-of-flight (TOF) mass spectrometry. A strong nonlinear dependence of the amount of desorbed C^+ ions on laser fluence is interpreted by the mechanism that C^+ ions are produced directly from the graphite via conversion of the multiphoton energy into thermal energy. The temporal evolution of C^+ ions was measured by varying the delay time of the ion repelling pulse with respect to the laser irradiation, which provides significant information on the ablated plume characterization. The TOF distributions of ablated ions showed a bimodal shape and could be fitted by shifted Maxwell-Boltzmann distributions. The velocity of the fast component increases with the delay time, whereas the slow component (< 500 m/s) exhibits a constant velocity. Also studied were the effects of the laser fluence on the energetics of C^+ ions.

Introduction

Pulsed laser ablation provides a convenient method for processing a wide variety of solid materials. Recently, laser ablation of graphite target has proved to be one of the most suitable methods for the thin film preparation of fascinating materials like fullerenes, single-walled nanotubes, and diamond like carbon (DLC) films.[1-3] In order to produce high quality films with unique characteristics, however, it is desirable to know the composition and energetics of the particles being deposited and to understand the mechanisms that produce these particles.

An understanding of the temporal behavior of ejected species in the ablated plume is important in order to deposit thin film with desired properties. Although laser-ablated plasmas have been studied to some extent, the dynamics of laser interaction with materials as well as the detailed aspects of laser-induced plume formation and expansion are not fully understood, particularly in the case of carbon. Studying the spatial and velocity distribution of the ablated species, particularly during initial ejection and expansion, can provide a better knowledge of the ablation dynamics.

A detailed understanding of the elementary processes in the irradiated material leading to ablation, as well as the interactions in the plume occurring after the ejection events, is essential for characterization of the final velocity distribution. Several experimental studies such as emission spectroscopy,[4] optical absorption spectroscopy,[5] laser-induced fluorescence spectroscopy,[6,7] time-integrated and time-resolved imaging,[8] and time-of-flight mass spectroscopy techniques[9,10] were applied to clarify the nature of the ablated plume. There is no clear understanding, however, of the physical processes leading to the observed time dependent velocity profile of the ejected particles since laser ablation is a transient process involving complex physical phenomena.

In this work our emphasis is on elucidating the details of the C^+ laser ablation mechanism and its temporal propaga-

tion dynamics. The laser-induced plume from the graphite target in a high vacuum condition are characterized by measuring their TOF mass spectra and obtaining time dependent velocity profiles using a pulsed-field time-of-flight mass spectrometric technique. We show that when the observed correlation between the spatial and velocity distributions is transformed into a relation of arrival time of TOF mass spectra, the flow velocity of ejected ionic species can be determined. The flow dynamics of plume expansion as well as the ablation mechanism are also investigated as a function of laser fluence.

Experimental Section

The experimental apparatus for laser ablation/pulsed-field TOFMS system was reported previously.[10,11] Briefly, laser ablation of a graphite target was carried out in a vacuum chamber (base pressure $< 5 \times 10^{-7}$ Torr) combined with a TOFMS, where positive ions were accelerated by a pulsed electric field and detected with a microchannel plate (MCP) detector. A target disk (10 mm in diameter, 2.5 mm thick) of graphite (99.95% purity) was placed at the repeller of the ion optics. A laser beam at 355 nm provided by the third harmonic of a Q-switched Nd : YAG laser is focused and is irradiated on the target with an angle 45° normal to the surface. The laser fluence used in these experiments ranges from 0.51 to 0.96 J/cm^2 with a pulse duration of 10 ns and repetition rate of 10 Hz. Following a delay of typically $\tau_d = 0\text{-}1.0$ μs after the laser shot, the positive ions are extracted by a +1500 V pulsed electric field, applied to the repeller, and enter the 1-mm small orifice of the collecting electrode. The ion signal from MCP detector is recorded by a 300 MHz digital oscilloscope (LeCroy 9350A), which is interfaced to an IBM computer. The mass spectra in the present experiment are obtained by a cumulative collection of 300 laser shots.

The TOF mass spectrometer can be operated in two modes depending on the delay time of the pulsed repelling field. In

mass spectrometer mode, the ions are accelerated without delay time ($\tau_d = 0$) right after the laser ablation, thus the mass spectrum can be obtained. In the translational spectrometer mode, the velocity distribution of the ablated ions can be determined by measuring its TOF distribution at a variable τ_d with respect to the timing of the laser pulse. Since the ions in the ejected plume propagate in the field-free region of the source during the delay time τ_d, the velocity components at directions normal to the ablation surface can be calculated from the arrival time of ion, the delay time τ_d, and the geometric parameters of mass spectrometer.[11,12] This method thus reflects the spatial and velocity distribution of ions above the target surface.

Results and Discussion

Figure 1 illustrates a typical TOF mass spectrum of cations produced by 355 nm laser irradiation on a graphite target in high-vacuum with a laser fluence of 0.51 J/cm². The spectrum is obtained with the mass spectrometer mode ($\tau_d = 0$ ms). It exhibits a major sequence of carbon cluster ions up to twenty atoms. The intensity distribution is nearly identical to that observed at low laser fluence (< 1 J/cm²) of $\lambda = 532$ nm by Gaumet *et al.*[13] In addition, intensity alterations with higher intensities of C_{11}^+ and C_{15}^+ peaks are similar to those for laser ablation followed by a supersonic expansion with helium gas.[14] Eyler, *et al.* measured the ionization potentials (IP's) of carbon clusters on the basis of charge-transfer technique.[15,16] These authors found that the odd-numbered carbon clusters represent each minimum in a plot of IP's over the cluster size. The unusual abundance of these cluster ions may thus be due to their low IPs rather than to a special degree of stability. The relatively low dissociation energies of even-numbered cluster ions also reveal the *n*-odd species to be more stable than the *n*-even species for *n* = 1-15.[17]

It is also found that the laser fluence changes drastically the relative intensity distribution of cluster ions. The enhancement of the C_1^+ and C_3^+ ion signals becomes more prominent as the laser fluence is increased, indicating that the concen-
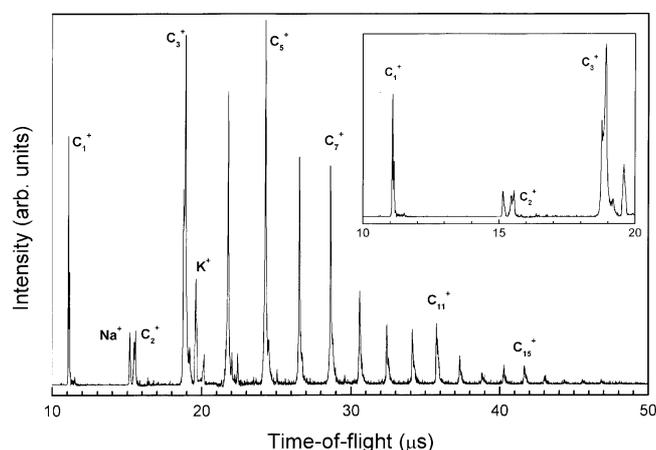
tration of the small cluster ions increases with laser fluence mainly due to the fragmentation of larger clusters within the hot plume. Therefore, it is believed that fragmentation process is much faster than the time scale of plume propagation after the laser irradiation. The peaks at 15.1 μs and 19.6 μs correspond to the trace impurity elements, known to exist in the graphite target surface, such as Na and K. Both elements were used as internal references for the mass calibration.

The inset of Figure 1 represents the expanded TOF mass spectrum corresponding to C_1^+-C_3^+ ions. As can be seen from the spectrum, each peak of monatomic and cluster ions shows a bimodal distribution, which is ascribed to the two different velocity components of ablated ions. The peaks at longer and shorter TOF correspond to the slow and fast velocity component, respectively, as will be described in more detail later. The fact that different velocity components are obtained for same mass clearly reveals the formation of two separated ionic clouds during the plume formation and expansion.

In order to understand the ablation mechanism of C^+ ions, the effect of laser fluence at the target surface was investigated over a range of 0.51-0.96 J/cm². Figure 2 displays the TOF spectra of laser ablated C^+ ions in high vacuum as a function of the laser fluence. The delay time between the laser shot and the ion extraction pulse was set at $\tau_d = 0$ μs. The signal intensities obtained at $\Phi = 0.51$ J/cm², 0.64 J/cm², and 0.80 J/cm² were increased by the factor of 20, 15, and 5 to facilitate comparison. Increasing the laser fluence, the spectra are characterized by the increase of ion intensities, indicating that more materials are ablated and emitted from the target. The temporal distribution of ions in each spectrum exhibits quite a broad distribution as the laser fluence increases.

Another distinct feature to be noted is that each TOF spectrum consists of two components, which correspond to fast and slow velocity component. Furthermore, it is observed that increasing the laser fluence, the arrival time of fast component keeps getting short while the slow component shifts toward the longer flight time. The peak width also becomes
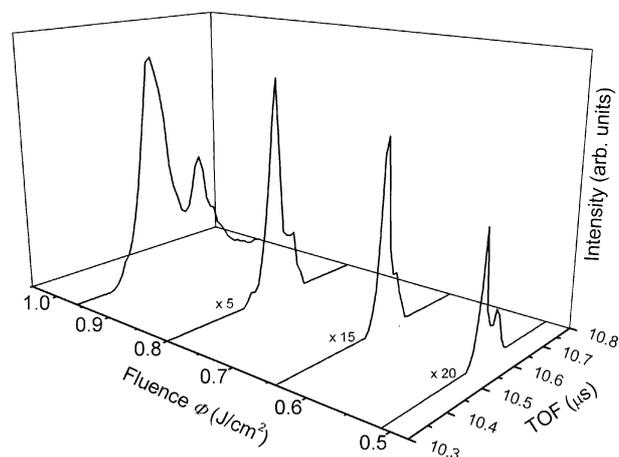

Figure 1. Typical TOF mass spectrum of laser ablated ions produced by laser irradiation ($\lambda = 355$ nm) of a graphite target in high vacuum. The laser fluence is 0.51 J/cm².

Figure 2. Time-of-flight spectra of laser ablated C^+ ions in high vacuum as a function of laser fluence at $\tau_d = 0$ μs. The signal intensities $\Phi = 0.51$ J/cm², 0.64 J/cm², and 0.8 J/cm² were increased by the factor of 20, 15, and 5 to facilitate comparison.

more and more wide. This behavior can be ascribed to the Coulomb interaction of ions and electrons inside the plume. As the energy density is raised, more material is ablated from the target and the plume density is increased. For this reason, the Coulomb repulsion of ions within the dense plume as well as the Coulomb attraction of the ions by negatively charged electrons escaping from the plume boundary will be increased. Therefore, the fast velocity component is accelerated forward, and the slow one is moving backward at directions normal to the ablation surface.

The ion intensity increases nonlinearly with laser fluence, *i.e.*, $I = aF^q$, where I is the integrated C^+ signal, a is a constant, and F is the laser fluence. Because the power law is characteristic for a multiphoton process, we consider that the ablation of C^+ ion is caused by the q-photon process at the present fluence range of 0.51-0.96 J/cm². From the best linear fit of the log$I$ versus logΦ plot, $q = 6.5$ is obtained. Only 4 photons ($h\nu = 3.5$ eV) are sufficient for ionization of valence shell electron, considering the ionization potential of carbon monovalent ion ($E_{IP} = 11.3$ eV).[18] For the formation energy of C^+ ions, $E(C^+)$, from the graphite surface, however, the bond-breaking energy $E_d(C)$ of a carbon atom from an atomic monolayer composed of sp^2 bonding character should be taken into account, *i.e.*, $E(C^+) = E_d(C) + E_{IP}$.[12] The calculated number of photons necessary for generating C^+ ions is found to be $q = 5.3$. The discrepancy between the observed q value with theoretical value is presumably due to the additional photofragmentation of high cluster ions during the nanosecond laser pulse, which results in an additional increase of C^+ ions at high laser fluence.

The pulsed-field time-of-flight mass spectrometric technique, which observes the TOF ion signal as a function of the delay time between the laser shot and the repelling electric field applied, offers an excellent means to investigate the distribution of the ionic species at the initial stage of plume expansion. The TOF spectra corresponding to the C^+ ions were plotted as a function of the delay time, as shown in Figure 3. The spectra were obtained with laser pulse energy of 0.96 J/cm². An increase in the delay time results in a small decrease of ion intensities, indicating that the ablated plume does not spread greatly in space above the target surface during the delay time of current study. The result is consistent with the previous observations that the expansion of the plume is one dimensional during shorter time intervals while for larger time scales the expansion is essentially three dimensional.[19] The maximum peak intensity at $\tau_d = 0.07$ μs is attributed to the narrow peak width of the spectrum due to the space focusing effect of linear TOFMS.[20] Its integrated intensity is, however, smaller than those of spectra at $\tau_d = 0$-0.05 μs region.

Another important observation is that each TOF spectrum consists of two components as a result of the two separated ionic clouds. The arrival times of each component shift to a longer flight time with increasing τ_d. This is because the ions move away from the target surface during τ_d, thus acquire less kinetic energy U after repelling electric field is applied. In addition, it is also noted that the arrival time of the fast
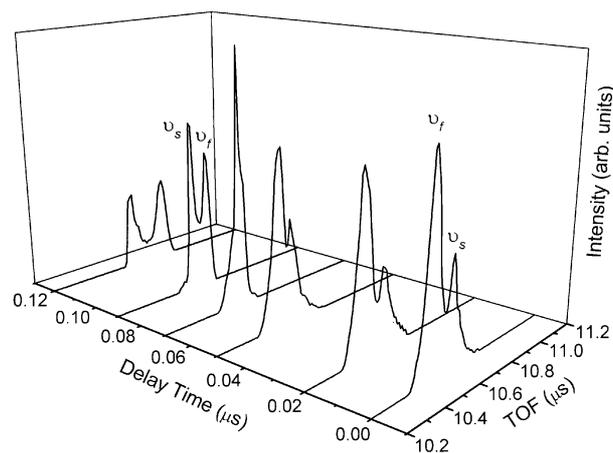

Figure 3. TOF spectra of laser ablated C^+ ions in high vacuum as a function of delay time between the laser shot and the extraction pulse. The laser fluence is 0.96 J/cm². υ_s and υ_f denote the slow and fast velocity components, respectively.

velocity component (υ_f) is shorter than that of slow one (υ_s) at $\tau_d \leq 0.05$ μs. The observation of the single peak structure at $\tau_d = 0.07$ μs is indicative of the same arrival time of two velocity components in spite of their different positions after the plume expansion. This space focusing is due to the fact that an ion initially closer to the ion detector (fast expansion velocity) acquires less energy within the repelling electric field and is therefore eventually overtaken by ions that have slow expansion velocity. After $\tau_d = 0.08$ ms the twin peak structure of the TOF spectra appears again, where the arrival time of the fast component shows a longer flight time than that of the slow one.

It is interesting to note that the two kinds of the velocity distributions can be distinguished in each spectrum, suggesting that the particles emitted on the surface of the target are separated into two components at the early stage of the ablation. This phenomena are also observed with the continuous extracting field, *i.e.*, $\tau_d = 0$, which means that the bimodal peak shapes are not affected by the experimental conditions. The observation of two velocity components may be caused either by a delayed emission of ejecta after the laser irradiation or by the hydrodynamic effects within the ablated plume. Namely, higher fluence than the critical energy density may produce ions deep inside the solid that exhibit some time-delay because of collisions with ions desorbed from the surface region. In Figure 3, the arrival time of C^+ ion is distributed in the range 10.4-10.8 μs at $\tau_d = 0$. If the two velocity components could be ascribed to the delayed emission of C^+ ions with the same velocity distribution, the broad arrival time distribution with increasing τ_d would be expected due to the spatial spread of ions during the delay time after the laser shot. The observation of the narrower peak width of C^+ ions at $\tau_d = 0.05$-0.1 μs region eliminates the possibility of delayed emission of ablated ions.

In a fast intensified-CCD photographic studies on the laser ablation of YBCO target, Geohegan has reported that the fast component expands nearly one-dimensionally and the slow, stationary component occupies a region out to $d \cong 1$

mm from the target surface.[21,22] Kelly *et al.* have also suggested that the collisions between the ejected species during the initial expansion produce a stopped or backward-moving component close to the target and a strongly forward-peaked velocity component away from the target.[23,24] These results are in reasonable agreement with our current observation since there is ample time for the particles to undergo collisions within the plume during the nanosecond duration of the laser pulse. It is, therefore, concluded that the accelerated motion of the ions at the front side of the plume slow down the ions that ablate near the end of the laser pulse.

As another possible route that could produce the two velocity components of C^+ ions could involve the different formation processes of ejected species. The C^+ ions formed by the direct ablation have, in general, larger translational energy than neutral atoms due to the charge separation induced by the electrons escaping from the plume boundary. The slow velocity component might come from the ions formed by either fragmentation of the larger cluster ions or collisional ionization of neutral atoms.

The TOF spectra taken at different delay time enable us to deduce the time-dependent kinetic energy information of ablated ions at the initial stage of plume expansion. The arrival time distribution of C^+ ion can easily be transformed into velocity distribution using a shifted Maxwell-Boltzmann (MB) distribution.[11,12] In fact, due to collisions among the evaporated particles in the first stage of plume expansion in vacuum, laser ablation from solid surface behaves like a nozzle source, creating a strongly forward-peaked particle flux with a large center of mass velocity υ_z along the normal to the target surface. For the bimodal distributions that we observe the fit function is of the form[25]

$$f(\upsilon_z) = A\upsilon_z^3 \exp[-m(\upsilon_z-\upsilon_s)^2/2kT_s] + B\upsilon_z^3$$
$$\exp[-m(\upsilon_z-\upsilon_f)^2/2kT_f] \quad (1)$$

where $\upsilon_{s,f}$ denote the flow velocities and $T_{s,f}$ the translational (or stream) temperatures for the slow and fast components, respectively, m is the mass number of species, k is the Boltzmann constant, and A and B are parameters used to fit the relative intensities of the two components.

Figure 4 shows the results of the best curve fit (closed circles) and experimental TOF spectra (solid lines) of C^+ ion with a laser fluence of 0.96 J/cm^2 at τ_d = 0.09 and 0.14 μs. Each peak in the TOF spectra is well fitted by a shifted MB distribution of ejected ions given in Eq. (1), implying that the ions desorbed by the laser ablation reach thermal equilibrium at each expansion stage. Such thermal equilibrium results from many collisions between ions because the ion density is very high at the early stage of the ion flight. The results also indicate that the expansion process of ionic species in the plume is similar to that of the supersonic nozzle expansion.[26] The fast and slow flow velocities at τ_d = 0.09 μs are determined to be 2090 m/s and 410 m/s, respectively. At τ_d = 0.14 μs, the fast velocity in the plume is increased to 3990 m/s. The errors of stream velocities are found to be in the range of ±20 m/s.

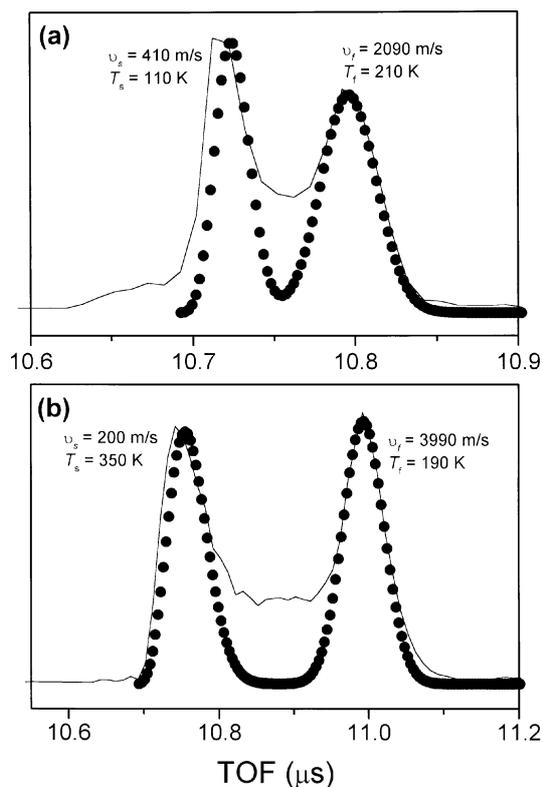The large arrival time difference of 0.13 μs between the

Figure 4. The shifted Maxwell-Boltzmann fit of the TOF spectra of C^+ ion with a laser fluence of 0.96 J/cm^2 at (a) τ_d = 0.09 and (b) τ_d = 0.14 ms. The solid lines are experimental data and the closed circles are the best fit. Fit parameters (a) T_s = 110 K, υ_s = 410 m/s, T_f = 210 K, υ_f = 2090 m/s, (b) T_s = 350 K, υ_s = 200 m/s, T_f = 190 K, υ_f = 3990 m/s.

two peaks observed at zero delay time (see Figure 3) does not allow us to obtain a reliable fit for the velocity distribution. This is because these peaks correspond to C^+ ions with their initial velocity direction towards (the peak at shorter TOF corresponding to positive υ_z) and away from (the peak at longer TOF corresponding to negative υ_z) the detector. The double peaks at τ_d = 0 thus can only be explained in terms of a Coulomb repulsion between the ions within an high-density cloud close to the surface in the very early stage of ablation. In this reason, the theoretical fit of TOF data at short delay time of less than 0.02 μs does not provide any meaningful information on the flow velocity and its distribution.

The time resolved observation presented here characterizes the axial expansion of the plume, *i.e.*, strictly along a direction perpendicular to the target surface. The flow velocities $\upsilon_{s,f}$ of C^+ ions, plotted as a function of delay time at different laser fluences of 0.51 J/cm^2 and 0.96 J/cm^2, are represented in Figure 5. It is quite interesting to note that at 0.51 J/cm^2 the flow velocity of fast component increases rapidly with delay time showing a free expansion behavior and reaches a plateau (υ_f = 2400 m/s) after τ_d = 0.09 μs. On the other hand, that of slow velocity component (less than 500 m/s) remains almost unchanged. The increase in the fast velocity component can be a result of the increased temperature and pressure of the plume formed above the target sur-
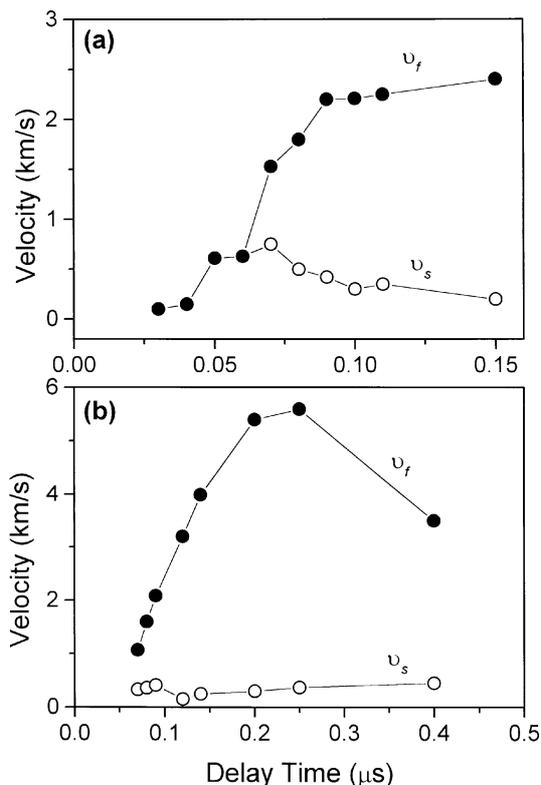
Figure 5. The flow velocity of C^+ ions as a function of delay time between the laser irradiation and the extraction pulse at (a) 0.51 J/cm^2 and (b) 0.96 J/cm^2 laser fluence.

face. Initially, the expansion is isothermal during the time interval of the laser pulse. After the laser pulse terminates, the plasma expands adiabatically in the vacuum and the thermal energy of the plasma is converted into kinetic energy. The plasma cools rapidly and the stream velocity starts to increase.

At high laser fluence of 0.96 J/cm^2, the increasing tendency of the fast velocity with the delay time is similar to that of Figure 5(a) but its maximum velocity is substantially increased to 5600 m/s. This is because the higher-energy density leads to a higher initial temperature of the plasma, which in turn gives rise to higher plume velocities. The sudden decrease in the velocity of these species after 0.3 μs, however, shows the deceleration of the C^+ species after a long delay time.

Conclusion

The pulsed-field TOFMS technique was used to characterize the temporal evolution of C^+ ions in a laser ablated plume produced by irradiating a graphite target at different laser fluences, with an Nd:YAG laser operating at 355 nm. The obtained relationship between the amount of ions and the laser fluence indicates that the ablation is caused by multiphoton process when λ = 355 nm laser is used as a light source. The TOF distributions of C^+ ions are simulated very well by a shifted Maxwell-Boltzmann distribution superimposed on a flow velocity. The time resolved analysis of the ablated ions shows the two velocity distributions with the

fast (1000-6000 m/s) and slow (< 500 m/s) components, indicating that the ablated species emitted above the target surface separates into two components during plume propagation. It is also found that the fast velocity component is greatly affected by the laser fluence as well as the delay time after the laser irradiation.

References

1. Kroto, H. W.; Heath, R. J.; Brien, S. C.; Curl, R. F.; Smalley, R. E. *Nature* **1985**, *318*, 165.
2. Iijima, S.; Ichihashi, T. *Nature* **1993**, *363*, 603.
3. Lowndes, D. H.; Geohegan, D. B.; Puretzky, A. A.; Norton, D. P.; Rouleau, C. M. *Science* **1996**, *273*, 898.
4. Tasaka, Y.; Tanaka, M.; Usami, S. *Jpn. J. Appl. Phys.* **1995**, *34*, 1673.
5. Geohegan, D. B.; Mashburn, N. D. *Appl. Phys. Lett*. **1989**, *55*, 2345.
6. Kunudumi, W. K. A.; Nakayama, Y.; Nakata, Y.; Okada, T.; Maeda, M. *Jpn. J. Appl. Phys.* **1993**, *32*, L271.
7. Okada, T.; Shibamaru, N.; Nakayama, Y.; Nakata, Y.; Maeda, M. *Appl. Phys. Lett.* **1992**, *60*, 941.
8. Geohegan, D. B.; Puretzky, A. A. *Appl. Phys. Lett.* **1995**, *67*, 197.
9. Creasy, W. R.; Brenna, J. T. *J. Chem. Phys*. **1990**, *92*, 2269.
10. Choi, Y. K.; Im, H.-S.; Jung, K.-W. *Bull. Korean Chem. Soc.* **1998**, *19*, 829.
11. Choi, Y. K.; Im, H. S.; Jung, K. W. *Appl. Surf. Sci.* **1999**, *150*, 152.
12. Choi, Y. K.; Im, H. S.; Jung, K. W. *Int. J. Mass Spectrom.* **1999**, *189*, 115.
13. Gaumet, J. J.; Wakisaka, A.; Shimizu, Y.; Tamori, Y. *J. Chem. Soc., Faraday Soc.* **1993**, *89*, 1667.
14. Rohlfing, E. A.; Cox, D. M.; Kaldor, A. *J. Chem. Phys.* **1984**, *81*, 3322.
15. Ramanathan, R.; Zimmerman, J. A.; Eyler, J. R. *J. Chem. Phys.* **1993**, *98*, 7838.
16. Bach, S. B.; Eyler, J. R. *J. Chem. Phys.* **1989**, *92*, 358.
17. Sowa-Resat, M. B.; Hintz, P. A.; Anderson, S. L. *J. Phys. Chem.* **1995**, *99*, 10736.
18. Raghavachari, R.; Binkley, J. S. *J. Chem. Phys.* **1987**, *87*, 2191.
19. Gupta, A.; Baren, B.; Casey, K. G.; Husley, B. W.; Kelly, R. *Appl. Phys. Lett.* **1991**, *59*, 1302.
20. Wiley, W. C.; McLaren, I. H. *Rev. Sci. Instrum.* **1955**, *26*, 1150.
21. Geohegan, D. B. *Appl. Phys. Lett.* **1992**, *60*, 2732.
22. Geohegan, D. B. *Laser Ablation of Electronic Materials: Basic Mechanisms and Applications*; Fogarassy, E., Lazare, S., Eds.; North-Holland: Amsterdam, 1992.
23. Kelly, R.; Braren, B. *Appl. Phys. B* **1991**, *53*, 160.
24. Kelly, R. *J. Chem. Phys.* **1990**, *92*, 5047.
25. Zheng, J. P.; Huang, Z. Q.; Shaw, D. T.; Kwok, H. S. *Appl. Phys. Lett.* **1988**, *53*, 534.
26. Anerson, J. B.; Andres, R. P.; Fenn, J. B. *Adv. Chem. Phys.* **1966**, *10*, 275.